Eighth International Conference on
Geometry, Integrability and Quantization
June 9–14, 2006, Varna, Bulgaria
Ivaïlo M. Mladenov and Manuel de León, Editors
SOFTEX, Sofia 2007, pp 246–263

THE MYLAR BALLOON: NEW VIEWPOINTS AND GENERALIZATIONS

IVAÏLO M. MLADENOV and JOHN OPREA†

Institute of Biophysics, Bulgarian Academy of Sciences
Acad. G. Bonchev Str., Bl. 21, 1113 Sofia, Bulgaria

†*Department of Mathematics, Cleveland State University, 44115 Cleveland, U.S.A.*

Abstract. Elsewhere we gave a parametrization of the Mylar balloon in terms of elliptic functions. Here, we parametrize other linear Weingarten surfaces using the incomplete Beta function *and* the hypergeometric function. We also provide a corresponding variational characterization and Maple procedures which plot the linear Weingarten surfaces.

1. Introduction

Since the publication of [10], various authors (e.g., [2] and [5]) have studied balloon shapes from different perspectives. In this paper, we want to do two things: first, we want to derive the Mylar balloon from physical principles (based on [2] and [5]); secondly, we want to view the Mylar balloon as a specific example of a linear Weingarten surface and show how a specific parametrization may be derived, both from the defining geometric condition and from a variational problem generalizing the one characterizing the balloon.

The principal curvatures, k_1, k_2, at a point on a surface are the maximum and minimum curvatures of curves through the point obtained by slicing the surface with planes spanned by a chosen tangent vector and the unit normal of the surface at the point. There are certain situations where imposing a condition on principal curvatures characterizes a surface M. For instance, if we require that $k_1 = k_2$ at every point of a compact surface M, then M is a sphere (see [11, Theorem 3.5.1]). If we insist that M be a surface of revolution for which $k_1 = -k_2$, then the mean (or average) curvature vanishes: $H = (k_1 + k_2)/2 = 0$. Hence, M is a *minimal* surface of revolution. The only non-planar surfaces of this kind are *catenoids*,

surfaces obtained by revolving $y = a\cosh(x/a)$ (for a constant a) about the x-axis (see [12, Theorem 3.2.5]). More generally, if we require M to be a surface of revolution and $k_1 = -k_2 + c$, where c is a nonzero constant, then M is a surface of Delaunay (see [3] and [12]): that is, a surface of revolution with constant mean curvature. In this work, we consider surfaces with $k_1 = ck_2$: the *linear Weingarten surfaces*. As stated above, we will give explicit parametrizations for these surfaces in terms of certain special functions as well as giving a variational characterization of these surfaces analogous to the one given for the Mylar balloon in [10].

2. Some Differential Geometry

Before we can explore the Mylar balloon and its generalization, we need to review some topics in differential geometry. (Modern expositions of the subject can be found in, for instance, [7] and [11].) A parameterized surface $\mathcal{S}$ in $\mathbb{R}^3$ is given by a smooth vector-valued mapping $\mathbf{x}\colon D \to \mathbb{R}^3$,

$$\mathbf{x}(u, v) = (x(u, v), y(u, v), z(u, v))$$

where D is some domain in $\mathbb{R}^2$. The surface $\mathcal{S}$ is determined (locally) by its first and second fundamental forms

$$I = E\,\mathrm{d}u^2 + 2F\,\mathrm{d}u\,\mathrm{d}v + G\,\mathrm{d}v^2, \qquad II = \ell\,\mathrm{d}u^2 + 2m\,\mathrm{d}u\,\mathrm{d}v + n\,\mathrm{d}v^2$$

whose coefficients are given by

$$E = E(u, v) = \mathbf{x}_u \cdot \mathbf{x}_u, \quad F = F(u, v) = \mathbf{x}_u \cdot \mathbf{x}_v, \quad G = G(u, v) = \mathbf{x}_v \cdot \mathbf{x}_v$$
$$\ell = \ell(u, v) = \mathbf{x}_{uu} \cdot \mathbf{n}, \quad m = m(u, v) = \mathbf{x}_{uv} \cdot \mathbf{n}, \quad n = n(u, v) = \mathbf{x}_{vv} \cdot \mathbf{n}.$$

Here $\mathbf{n}$ is the unit normal vector to $\mathcal{S}$:

$$\mathbf{n} = \mathbf{n}(u, v) = \frac{\mathbf{x}_u \times \mathbf{x}_v}{|\mathbf{x}_u \times \mathbf{x}_v|}.$$

(We assume that $\mathbf{x}_u \times \mathbf{x}_v$ never vanishes in D.) Intuitively, the *metric coefficients* E, F, and G describe the stretching necessary to map a piece of the plane smoothly up to the surface under the parametrization. As can be seen from the definition, the coefficients ℓ, m, and n of II have more to do with acceleration and, hence, curvature. Indeed, there are classical formulas that describe two types of curvatures at every point of the surface. These are the **Gauss** and **mean** curvatures, denoted by K and H, respectively. The formulas are:

$$K = \frac{\ell n - m^2}{EG - F^2}, \qquad H = \frac{En + G\ell - 2Fm}{2(EG - F^2)}. \tag{1}$$

For a unit tangent vector $\mathbf{u}$ to $\mathcal{S}$ in $\mathbb{R}^3$ (at a point p of $\mathcal{S}$), the **normal curvature** $k(\mathbf{u})$ of $\mathcal{S}$ in the $\mathbf{u}$-direction is computed by slicing the surface with the plane

determined by $\mathbf{u}$ and the unit normal $\mathbf{n}$ and taking the curvature (at p) of the intersection curve. (In some sense, this is the most fundamental type of curvature associated with a surface.) This process defines a continuous real-valued function on the circle, $k\colon S^1 \to \mathbb{R}$ (where we identify unit vectors in $\mathbb{R}^2$ with the circle S^1). Because S^1 is compact, k attains both a maximum value k_1 and a minimum value k_2. These are called **principal curvatures** of $\mathcal{S}$ at p. It is known that $K = k_1 k_2$ and $H = (k_1 + k_2)/2$ (see [11]). From these equations, it is easy to derive the relations

$$k_1 = H + \sqrt{H^2 - K} \qquad \text{and} \qquad k_2 = H - \sqrt{H^2 - K}. \tag{2}$$

We deal only with surfaces of revolution that admit parametrizations of the general form (up to permutation of coordinates)

$$\mathbf{x}(u, v) = (r(u)\cos v, r(u)\sin v, z(u)). \tag{3}$$

It is easy to verify that for such a surface we always have $F = 0 = M$, so the formulas for Gauss and mean curvatures reduce accordingly. The principal curvatures for a surface of revolution are given by

$$k_\mu = \frac{z''r' - z'r''}{(z'^2 + r'^2)^{3/2}}, \qquad k_\pi = \frac{z'}{h\sqrt{z'^2 + r'^2}}. \tag{4}$$

The subscripts μ and π stand for the tangent directions along a meridian and a parallel circle, respectively. In fact, the profile curve $(r(u), z(u))$ will have the property that $r(u)$ has an inverse function. With this in mind, we can parametrize the surface of revolution as follows.

$$\mathbf{x}(u, v) = (u\cos v, u\sin v, z(u)). \tag{5}$$

The principal curvatures for a surface of revolution with this type of parametrization are given by

$$k_\mu = \frac{z''}{(1 + z'^2)^{3/2}}, \qquad k_\pi = \frac{z'}{u\sqrt{1 + z'^2}}. \tag{6}$$

3. Linear Weingarten Surfaces of Revolution

A surface is a **linear Weingarten surface** if the principal curvatures obey a linear relation $k_1 = ck_2$ for some constant c (see [9]). If we take a surface of revolution parametrized as above by $\mathbf{x}(u, v) = (u\cos v, u\sin v, z(u))$, then we have the following characterization.

Theorem 1. *A surface of revolution M as in* (5) *such that $z(r) = 0$, $z'(u) < 0$, $\lim_{u\to r} z'(u) = -\infty$ and $k_\mu = ck_\pi$ (with $c > 0$) has a parametrization of the form*

$\mathbf{x}(u,v) = (u\cos v, u\sin v, z(u))$ *with*

$$z(u) = \frac{r}{c+1}F\left(\frac{1}{2}, \frac{c+1}{2c}; \frac{3c+1}{2c}; 1\right) - \frac{u^{c+1}}{c+1}F\left(\frac{1}{2}, \frac{c+1}{2c}; \frac{3c+1}{2c}; \left(\frac{u}{r}\right)^{2c}\right) r^{-c}$$

and where $F(p,q;w;z)$ *denotes the hypergeometric function.*

Proof: First, let us relate the principal curvatures using the parametrization alone. From (6), we have

$$\begin{aligned}\frac{\mathrm{d}}{\mathrm{d}u}(uk_\pi) = k_\pi + u\frac{\mathrm{d}}{\mathrm{d}u}(k_\pi) &= \frac{z'}{u\sqrt{1+z'^2}} \\ &\quad + u\frac{z''u(1+z'^2) - z'((1+z'^2)^{1/2} + uz'z''/(1+z'^2)^{1/2}}{u^2(1+z'^2)} \\ &= \frac{z'(1+z'^2) + z''u - z'(1+z'^2)}{u(1+z'^2)^{3/2}} = \frac{z''}{(1+z'^2)^{3/2}} = k_\mu.\end{aligned}$$

Now suppose that $k_\mu = ck_\pi$. We then have

$$\begin{aligned} ck_\pi &= \frac{\mathrm{d}(uk_\pi)}{\mathrm{d}u} = k_\pi + u\frac{\mathrm{d}k_\pi}{\mathrm{d}u} \\ (c-1)k_\pi &= u\frac{\mathrm{d}k_\pi}{\mathrm{d}u} \\ \frac{c-1}{u}\,\mathrm{d}u &= \frac{\mathrm{d}k_\pi}{k_\pi} \\ \ln(u^{c-1}) + d &= \ln(k_\pi) \\ b^c u^{c-1} &= k_\pi \end{aligned}$$

and therefore

$$\begin{aligned} b^c u^{c-1} &= \frac{z'}{u\sqrt{1+z'^2}} \\ b^c u^c\sqrt{1+z'^2} &= z' \\ b^{2c}u^{2c}(1+z'^2) &= z'^2 \\ \frac{b^{2c}u^{2c}}{1-b^{2c}u^{2c}} &= z'^2 \\ -\frac{b^c u^c}{\sqrt{1-b^{2c}u^{2c}}} &= z'(u) \end{aligned}$$

so that one ends with the formula for the profile curve

$$z(u) = \int_u^r \frac{b^c \tilde{u}^c \, \mathrm{d}\tilde{u}}{\sqrt{1 - b^{2c}\tilde{u}^{2c}}}.$$

Now, we have $\lim_{u \to r} z'(u) = -\infty$, so we see that $b = 1/r$ and we obtain

$$z(u) = \int_u^r \frac{\tilde{u}^c \, \mathrm{d}\tilde{u}}{\sqrt{r^{2c} - \tilde{u}^{2c}}}.$$

Finally, Maple calculates the indefinite integral to be the following

```
> g_c:=simplify(int(u^c/sqrt(r^(2*c)-u^(2*c)),u))
assuming(c>0,r>0);
```

$$g\_c := \frac{u^{(c+1)} \, \mathrm{hypergeom}\left(\left[\frac{1}{2}, \frac{c+1}{2c}\right], \left[\frac{3c+1}{2c}\right], u^{(2c)} r^{(-2c)}\right) r^{(-c)}}{c+1}.$$

We now put in the limits of integration and obtain the function $z(u)$.

```
> eval(g_c,u=r)-g_c;
```

$$\frac{r^{(c+1)} \, \mathrm{hypergeom}\left(\left[\frac{1}{2}, \frac{c+1}{2c}\right], \left[\frac{3c+1}{2c}\right], 1\right) r^{(-c)}}{c+1}$$
$$- \frac{u^{(c+1)} \, \mathrm{hypergeom}\left(\left[\frac{1}{2}, \frac{c+1}{2c}\right], \left[\frac{3c+1}{2c}\right], u^{(2c)} r^{(-2c)}\right) r^{(-c)}}{c+1}.$$

□

Remark 2. Maple also provides the following simplification in terms of the Gamma function

```
> simplify(eval(g_c,u=r))-simplify(g_c);
```

$$\frac{1}{2} \frac{r\sqrt{\pi}\,\Gamma\left(\frac{c+1}{2c}\right)}{c\,\Gamma\left(\frac{2c+1}{2c}\right)} - \frac{u^{(c+1)} \, \mathrm{hypergeom}\left(\left[\frac{1}{2}, \frac{c+1}{2c}\right], \left[\frac{3c+1}{2c}\right], u^{(2c)} r^{(-2c)}\right) r^{(-c)}}{c+1}.$$

It is possible to place Theorem 1 into a broader context. Every soap film is a physical model of a minimal surface (but not conversely) and soap films arise from the variational principle of minimizing "energy" in the form of surface area (see [12]). Soap films also obey a relation known as the Laplace–Young equation, which asserts that the (gas) pressure difference across a film is proportional to the mean curvature, with proportionality constant the surface tension of the film. Of course, a film has the same pressure on both sides, so the mean curvature is zero and $k_1 = -k_2$. A natural question that arises is whether there are variational characterizations of surfaces satisfying restrictions $k_1 = ck_2$ for $c \neq -1, 1, 2$? Furthermore, we might ask if there are there any physical processes that produce these restrictions through a non-variational formulations?

In the following section we will answer the last question in the affirmative by outlining a mathematical model that we can use to formulate the problem of finding the equilibrium shape of strained balloons.

4. Modelling Balloon Shapes

So, now let us model a balloon physically. As usual, the axisymmetric balloon surface $\mathcal{S}$ will be determined by specifying its meridional section, a curve $s \longrightarrow (r(s), z(s))$ in the XOZ plane, where s is the natural parameter provided by the corresponding arclength. We will denote the total arclength by L. The surface $\mathcal{S}$ can be represented in ordinary Euclidean space $\mathbb{R}^3$, with a fixed orthonormal basis $(\mathbf{i}, \mathbf{j}, \mathbf{k})$, by making use of the parameter u and the angle v specifying the rotation of the XOY plane via the vector-valued function

$$\mathbf{x}(s, v) = r(s)\mathbf{e}_1(v) + z(s)\mathbf{e}_3(v), \qquad 0 < s \leq L, \quad 0 \leq v < 2\pi. \tag{7}$$

Here the vector $\mathbf{e}_1(v)$ is the new position of $\mathbf{i}$ after a rotation by angle v

$$\mathbf{e}_1(v) = \cos v\mathbf{i} + \sin v\mathbf{j}. \tag{8}$$

Since the rotation is around the third axis, the the vector $\mathbf{k}$ representing it in (7) is a constant: that is, $\mathbf{e}_3(v) = \text{const} = \mathbf{k}$. The pair $\{\mathbf{e}_1, \mathbf{e}_3\}$ can be completed to the orthonormal basis set $(\mathbf{e}_1, \mathbf{e}_2, \mathbf{e}_3)$ in $\mathbb{R}^3$. The third vector $\mathbf{e}_2(v)$ is introduced as the cross product of the vectors $\mathbf{e}_3(v)$ and $\mathbf{e}_1(v)$

$$\mathbf{e}_2(v) = \mathbf{e}_3(v) \times \mathbf{e}_1(v) = \mathbf{k} \times \mathbf{e}_1(v) = -\sin v\mathbf{i} + \cos v\mathbf{j}.$$

A more detailed specification of the surface requires us to find some other important characteristics of the generating curve. This relies mostly on the derivatives of $\mathbf{x}(s, v)$. For instance, the tangent vector at each point of the generating curve is given by the first derivative with respect to u

$$\mathbf{t}(s, v) = \mathbf{x}_s(s, v) = r'(s)\mathbf{e}_1(v) + z'(s)\mathbf{k}. \tag{9}$$

Here and elsewhere in this section, a prime denotes a derivative with respect to the meridional arclength s. Let us also introduce $\theta(s)$, which measures the angle between the normal vector $\mathbf{n}$ and $\mathbf{k}$. Then, the coordinates $r(s)$ and $z(s)$ depend on $\theta(s)$ through the equations

$$r'(s) = \cos\theta(s) \tag{10}$$

$$z'(s) = -\sin\theta(s). \tag{11}$$

Using these equations, we can express the tangent vector as

$$\mathbf{t}(s, v) = \cos\theta(s)\mathbf{e}_1(v) - \sin\theta(s)\mathbf{k}. \tag{12}$$

By differentiating the last relation with respect to the parameter s we get

$$\mathbf{x}_{ss} = -\theta'(s)(\sin\theta(s)\mathbf{e}_1(v) + \cos\theta(s)\mathbf{k}). \tag{13}$$

Next, we compute the first and second order derivatives of $\mathbf{x}(s,v)$ upon v

$$\mathbf{x}_v = r(s)(\mathbf{e}_1(v))_v = r(s)\mathbf{e}_2(v) \tag{14}$$

$$\mathbf{x}_{vv} = r(s)(\mathbf{e}_2(v))_v = -r(s)\mathbf{e}_1(v) \tag{15}$$

and finally, the mixed derivative

$$\mathbf{x}_{sv} = \mathbf{x}_{vs} = \cos\theta(s)\mathbf{e}_2(v). \tag{16}$$

Another significant object that we will need to know is the outward normal vector $\mathbf{n}(s,v)$. We can represent it as the cross product of the vectors $\mathbf{t}(s,v)$ and $\mathbf{e}_2(v)$

$$\mathbf{n}(s,v) = \mathbf{t}(s,v) \times \mathbf{e}_2(v) = \sin\theta(s)\mathbf{e}_1(v) + \cos\theta(s)\mathbf{k}. \tag{17}$$

The last couple of relations are sufficient to obtain the coefficients of the first fundamental form of $\mathcal{S}$

$$E = \mathbf{x}_s^2 = 1, \qquad F = \mathbf{x}_s \cdot \mathbf{x}_v = 0, \qquad G = \mathbf{x}_v^2 = r^2(s) \tag{18}$$

and of the second fundamental form of $\mathcal{S}$

$$\ell = \mathbf{n} \cdot \mathbf{x}_{ss} = -\theta'(s), \quad m = \mathbf{n} \cdot \mathbf{x}_{sv} = 0, \quad n = \mathbf{n} \cdot \mathbf{x}_{vv} = -r(s)\sin\theta(s). \tag{19}$$

Having these, we can easily find the principal curvatures along the respective meridional and parallel directions

$$k_\mu = \ell/E = -\theta'(s) \qquad \text{and} \qquad k_\pi = n/G = -\frac{\sin\theta(s)}{r(s)}. \tag{20}$$

Then the mean curvature can be expressed as

$$H = \frac{1}{2}(k_\mu + k_\pi) = -\frac{1}{2}\left(\theta'(s) + \frac{\sin\theta(s)}{r(s)}\right). \tag{21}$$

5. Equilibrium Equations

The results obtained in the previous section will help us to find the shape's equilibrium conditions. For that purpose, we will consider the forces acting on the surface. The internal forces are

$$\mathbf{f}_1(s,v) = \sigma_m(s)\mathbf{t}(s,v) \qquad \text{and} \qquad \mathbf{f}_2(s,v) = \sigma_c(s)\mathbf{e}_2(v). \tag{22}$$

On the left hand side of equation (22), $\sigma_m(s)$ means the **meridional stress resultant** and on the right side, $\sigma_c(s)$ is the **circumferential stress resultant** (see [2] for more details). Let us mention that the situation when $\sigma_c(s) \equiv 0$ is referred to in ballooning literature as the **natural shape model**.

The external forces depend on the pressure and the density of the balloon's material, namely,

$$\mathbf{f}(s,v) = p(s)\mathbf{n}(s,v) - w(s)\mathbf{k}. \tag{23}$$

Here $p(s)$ is the hydrostatic differential pressure due to the difference between the densities of the gas inside the balloon and the ambient air and $w(s)$ is the weight density per unit area of the film. In most cases $w(s)$ is assumed to be constant.

By balancing the internal and external forces we end up with the following equilibrium equations:

$$(\sigma_m(s)r(s)\mathbf{t})_s - \sigma_c(s)\mathbf{e}_1(v) + r(s)\mathbf{f}(s,v) = 0. \tag{24}$$

The above vectorial equation can be projected onto $\mathbf{n}$ and $\mathbf{t}$ and this gives us:

$$(\sigma_m(s)r(s))\frac{\mathrm{d}\theta}{\mathrm{d}u} = -w(s)r(s)\cos\theta(s) - \sigma_c(s)\sin\theta(s) + p(s)r(s) \tag{25}$$

$$\frac{\mathrm{d}(\sigma_m r(s))}{\mathrm{d}u} = -w(s)r(s)\sin\theta(s) + \sigma_c(s)\cos\theta(s). \tag{26}$$

6. Our Heroes–Delaunay's Surfaces and the Mylar Balloon

Despite the fact that the above system of equations governing the shapes is highly nonlinear, we have been successful in finding a few exact solutions which will be presented below. These solutions are obtained by neglecting or constraining some of the parameters in the equilibrium equations. For instance, for the case of axisymmetric shapes with $\sigma_c \neq 0$ or $\sigma_c = 0$, we present two models whose solutions give rise to Delaunay and Mylar balloon surfaces respectively.

Let us start with the case where the film weight contribution is zero, $w(s) \equiv 0$. We therefore have from the equations (25) and (26) the system

$$-(\sigma_m(s)r(s))\frac{\mathrm{d}\theta(s)}{\mathrm{d}s} = \sigma_c(s)\sin\theta(s) - p(s)r(s) \tag{27}$$

$$\frac{\mathrm{d}(\sigma_m(s)r(s))}{\mathrm{d}s} = \sigma_c(s)\cos\theta(s). \tag{28}$$

Taking into account the geometrical relation (10), the second equation in this system implies that the meridional and circumferential stresses are constant and of the same magnitude, $\sigma_m(s) = \sigma_c(s) = \sigma = \text{const}$, while the first equation (27) can be recognized as the mean curvature of $\mathcal{S}$,

$$H = -\frac{p(s)}{2\sigma}. \tag{29}$$

If we continue with an examination of the case where the hydrostatic pressure is also a constant, $p(s) = p_o = \text{const}$, we end up with a surface of constant mean curvature:

$$H = -\frac{p_o}{2\sigma} = \frac{\hat{p}}{2} = \text{const}, \qquad \hat{p} = \frac{p}{\sigma}. \tag{30}$$

The surfaces of revolution with constant mean curvature were identified many years ago by Delaunay [3] using a genuine geometrical argument – they are just the

traces of the foci of the non-degenerate conics when they roll along a straight line in a plane (*roulettes* in French). On the other hand, these surfaces of revolution minimize surface area subject to having a fixed volume (as proved by Sturm [3, Appendix]). This observation reveals why these surfaces make their appearance as soap bubbles, liquid drops ([5, 12]), cells under compression ([8, 14]) and now as balloon shapes. The list of all of Delaunay's surfaces includes planes which have mean curvature zero, cylinders of radius R and mean curvature $H = 1/2R$, spheres of radius R and mean curvature $H = 1/R$, catenoids of mean curvature $H = 0$, and nodoids and unduloids of constant non-zero mean curvatures.

Now let us consider another case in which the system of equations (25) and (26) can be solved completely. Let us assume this time that $w(s) = \sigma_c(s) = 0$ and that the hydrostatic pressure $p(s) = p_o$ is a non-zero constant. Then the system formed by (25) and (26) reduces to the equations

$$(\sigma_m(s)r(s))\frac{\mathrm{d}\theta(s)}{\mathrm{d}s} = p_o r(s) \tag{31}$$

$$\frac{\mathrm{d}(\sigma_m(s)r(s))}{\mathrm{d}s} = 0. \tag{32}$$

The second equation above tells us that $\sigma_m(s)r(s)$ is a constant quantity. Following Gibbons [5], we introduce the meridional stress resultant $\mathring{\sigma}$ on the *equator* of the balloon (i.e., the points for which $z(s) = 0$ and $r(s) = a$, where a is the radius of the inflated balloon) and re-write the above integral in the form

$$\sigma_m(s) = \frac{a\mathring{\sigma}}{r(s)}. \tag{33}$$

This allows as to transform the first equation (31) as follows:

$$\frac{\mathrm{d}\theta(s)}{\mathrm{d}u} = \mathring{p}r(s), \qquad \mathring{p} = \frac{p_o}{a\mathring{\sigma}}. \tag{34}$$

If we combine this equation with (10) we get another purely geometrical relation

$$r^2(s) = \frac{2}{\mathring{p}}\sin\theta(s). \tag{35}$$

Gibbons [5] also noticed that, by re-writing (35) in the form

$$-\mathring{p}r(s) = -2\frac{\sin\theta(s)}{r(s)}, \tag{36}$$

it is fairly easy to see that the surface under consideration actually satisfies the Weingarten relation

$$k_\mu = 2k_\pi. \tag{37}$$

In [10] it was shown that this relation between principle curvatures characterizes the Mylar balloon uniquely:

Theorem 3. *If $\mathcal{M}$ is a surface of revolution for which $k_\mu = 2k_\pi$, the surface $\mathcal{M}$ is the Mylar balloon.*

7. A Variational Characterization

In this section, we give a variational characterization of linear Weingarten surfaces generalizing the Mylar balloon. Let us first review notions from the calculus of variations.

The calculus of variations deals with problems of the following sort: Find a function $y = y(x)$ for which the functional

$$J = \int_{x_0}^{x_1} G(x, y(x), y'(x))\,\mathrm{d}x$$

takes its minimum (or, more generally, has a critical value). A (famous) necessary condition for a minimizer $y(x)$ is the **Euler–Lagrange equation**

$$\frac{\mathrm{d}}{\mathrm{d}x}\left(\frac{\partial G}{\partial y'}\right) - \frac{\partial G}{\partial y} = 0.$$

A function $y(x)$ that satisfies the Euler–Lagrange equation is said to *extremize* J. If we wish to minimize $J = \int_{x_0}^{x_1} G(x, y(x), y'(x))\,\mathrm{d}x$ subject to an extra constraint $I = \int_{x_0}^{x_1} H(x, y, y')\,\mathrm{d}x$, then we take the Euler–Lagrange equation associated with the functional

$$K = \int_{x_0}^{x_1} G(x, y, y') + \lambda H(x, y, y')\,\mathrm{d}x.$$

The constant λ is called a **Lagrange multiplier**. See [11], for instance, for details.

Now let us formulate the variational problem that will give us Weingarten surfaces. Recall that the nth *moment* of a function $y = f(x)$ is given by

$$\int x^n f(x)\,\mathrm{d}x.$$

For a surface of revolution about the z-axis, $\mathbf{x}(u, v) = (u\cos v, u\sin v, z(u))$, the first moment of $z(u)$ is simply the volume of $\mathbf{x}(u, v)$ (up to a constant)

$$V = 4\pi \int_0^\tau uz(u)\,\mathrm{d}u. \tag{38}$$

Of course, the variational problem that gave rise to the Mylar balloon was to maximize volume subject to a fixed arclength for the profile curve. Of course, we also assumed that the profile curve $z(u)$ obeyed the conditions $z(r) = 0$, $z'(u) < 0$ and $\lim_{u\to r} z'(u) = -\infty$ as well. With this in mind, let us formulate the general problem:

$(c-1)$st Moment Problem. For a surface of revolution as described above, extremize the $(c-1)$th moment of $z(u)$

$$\int u^{c-1} z(u)\,\mathrm{d}u \tag{39}$$

subject to

$$\int_0^r \sqrt{1+z'(u)^2}\,\mathrm{d}u = a. \tag{40}$$

The corresponding constrained Euler–Lagrange equation is

$$\frac{\mathrm{d}}{\mathrm{d}u}\left(\frac{\lambda z'(u)}{\sqrt{1+z'(u)^2}}\right) - u^{c-1} = 0. \tag{41}$$

This equation is easy to integrate, yielding

$$\frac{\lambda z'(u)}{\sqrt{1+z'(u)^2}} = u^c + C \tag{42}$$

for some constant of integration C. This constant can be found by taking into account the obvious geometrical (transversality) condition $z'(0) = 0$. Inserting $u = 0$ into (42) and using $z'(0) = 0$ gives $C = 0$. Consequently, we obtain

$$\frac{z'(u)}{\sqrt{1+z'(u)^2}} = \frac{1}{\lambda}u^c. \tag{43}$$

The transversality condition $\lim_{u\to r^-} z'(u) = -\infty$, along with the requirement that the curve proceed from its highest point to its intersection with the u-axis without introducing critical points (i.e., $z'(u) < 0$ when $0 < u < r$), allows us to rewrite $1/\lambda$ in the form $-b^c$. Then, solving (43) for $z'(u)$, we find that

$$z'(u) = -\frac{u^c}{\sqrt{1-b^{2c}u^{2c}}}.$$

We also want $\lim_{u\to r^-} z'(u) = -\infty$, so we obtain $b = 1/r$. We then have

$$z(u) = \int_u^r \frac{\tilde{u}^c}{\sqrt{r^{2c}-\tilde{u}^{2c}}}\,\mathrm{d}\tilde{u}, \qquad 0 \le u \le r \tag{44}$$

where, again, the choice of the upper limit of integration comes from the requirement that $z(r) = 0$. But this is the function we found for a linear Weingarten surface with $k_\mu = nk_\pi$. Thus, we have the following

Theorem 4. *The surface of revolution $\mathcal{S}$ that solves the $(c-1)$st moment variational problem is a linear Weingarten surface parametrized as in Theorem 1 by*

$$\mathbf{x}(u,v) = \left(u\cos v, u\sin v, \left|_u^r \frac{u^{c+1}}{c+1} F\left(\frac{1}{2}, \frac{c+1}{2c}; \frac{3c+1}{2c}; u^{2c}r^{-2c}\right) r^{-c}\right.\right)$$

where $F(p,q;w;z)$ denotes the hypergeometric function.

Now that we have seen that the $(c-1)$st moment problem leads to linear Weingarten surfaces, we can ask the following fundamental question.

Question 5. What is the underlying physical meaning of the $(c-1)$st moment problem?

8. Using Maple to Visualize Weingarten Surfaces

We can now put this parametrization into a computer algebra system `Maple` and plot. We then see the shape of a linear Weingarten surface in Figure 1.

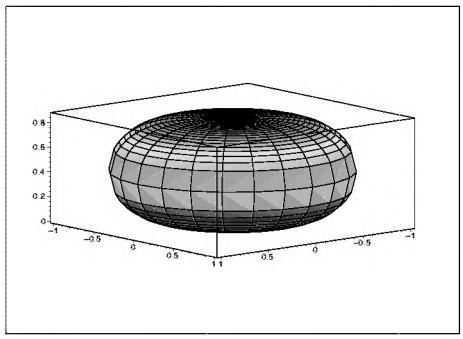

Figure 1. A linear Weingarten surface with $c = 3$.

The following Maple code plots linear Weingarten surfaces with input c the coefficient in $k_\mu = ck_\pi$. We also include a check that the ratio of principal curvatures is c. In order to do this, we need various procedures computing Gauss and mean curvatures, etc. Also, in order to plot the whole surface, we need to take this function and flip it about the u-axis. The complete Maple structure is:

```
> EFG := proc(X)
> local Xu,Xv,E,F,G;
> Xu := <diff(X[1],u),diff(X[2],u),diff(X[3],u)>;
> Xv := <diff(X[1],v),diff(X[2],v),diff(X[3],v)>;
> E := DotProduct(Xu,Xu,conjugate=false);
> F := DotProduct(Xu,Xv,conjugate=false);
> G := DotProduct(Xv,Xv,conjugate=false);
> simplify([E,F,G]);
> end:
```

The following procedure gives the unit normal **n** to the input surface `X`. If you wish to take `UN(X)`, then `X` must be given in parameterized form:

```
> UN := proc(X)
> local Xu,Xv,Z,s;
> Xu := <diff(X[1],u),diff(X[2],u),diff(X[3],u)>;
> Xv := <diff(X[1],v),diff(X[2],v),diff(X[3],v)>;
> Z := CrossProduct(Xu,Xv);
> s:=VectorNorm(Z,Euclidean,conjugate=false);
> simplify(<Z[1]/s|Z[2]/s|Z[3]/s>,sqrt,trig,symbolic);
> end:
```

The following gives the second fundamental form:

```
> lmn := proc(X)
> local Xu,Xv,Xuu,Xuv,Xvv,U,l,m,n;
> Xu := <diff(X[1],u),diff(X[2],u),diff(X[3],u)>;
> Xv := <diff(X[1],v),diff(X[2],v),diff(X[3],v)>;
> Xuu := <diff(Xu[1],u),diff(Xu[2],u),diff(Xu[3],u)>;
> Xuv := <diff(Xu[1],v),diff(Xu[2],v),diff(Xu[3],v)>;
> Xvv := <diff(Xv[1],v),diff(Xv[2],v),diff(Xv[3],v)>;
> U := UN(X);
> l := DotProduct(U,Xuu,conjugate=false);
> m := DotProduct(U,Xuv,conjugate=false);
> n := DotProduct(U,Xvv,conjugate=false);
> simplify([l,m,n],sqrt,trig,symbolic);
> end:
```

Finally we can calculate Gauss curvature K as follows:

```
> GK := proc(X)
> local E,F,G,l,m,n,S,T;
> S := EFG(X); T := lmn(X);
> E := S[1]; F := S[2]; G := S[3];
> l := T[1]; m := T[2]; n := T[3];
> simplify((l*n-m^2)/(E*G-F^2),sqrt,trig,symbolic);
> end:
```

Mean curvature is given by

```
> MK := proc(X)
> local E,F,G,l,m,n,S,T;
> S := EFG(X); T := lmn(X);
> E := S[1]; F := S[2]; G := S[3];
> l := T[1]; m := T[2]; n := T[3];
> simplify((G*l+E*n-2*F*m)/(2*E*G-2*F^2),sqrt,trig,
> symbolic);
> end:
```

The two principal curvatures of the surface are given by $k_1 = H + \sqrt{H^2 - K}$ and $k_2 = H - \sqrt{H^2 - K}$.

```
> princurv:=proc(X)
> local k1,k2;
> k1:=simplify(MK(X)+sqrt(MK(X)^2-GK(X)),symbolic);
> k2:=simplify(MK(X)-sqrt(MK(X)^2-GK(X)),symbolic);
> print('k_1=',k1,'k_2=',k2);
> end:
```

The following procedure plots the linear Weingarten surface corresponding to the parameter c. Note that we can only approach the boundary input 1. Also note that the procedure supplies output that checks numerically that the ratio of principal curvatures is the input parameter c. We suppress that output below simply to save space.

```
> linwein:=proc(c,r)
> local Xcbot,Xctop,top,bot,k1,k2,pc,profile_c;
> profile_c:=
> u^(c+1)*hypergeom([1/2,1/2*(c+1)/c],[1/2*(3*c+1)/c],
> u^(2*c)*r^(-2*c))*r^(-c)/(c+1);
> Xctop:=<u*cos(v)|u*sin(v)|eval(profile_c,u=r)
> -profile_c>;
> Xcbot:=<u*cos(v)|u*sin(v)|-(eval(profile_c,u=r)
> -profile_c)>;
> k1:=simplify(MK(Xcbot)+sqrt(MK(Xcbot)^2-GK(Xcbot)));
> k2:=simplify(MK(Xcbot)-sqrt(MK(Xcbot)^2-GK(Xcbot)));
> print('The ratio of the principal curvatures is',
> eval(k1/k2,u=0.1),eval(k1/k2,u=0.3),
> eval(k1/k2,u=0.5),eval(k1/k2,u=0.8));
> bot:=plot3d(Xcbot,u=0..0.9999999,v=0..2*Pi,shading
> =zhue,
> scaling=constrained, orientation=[50,80]);
> top:=plot3d(Xctop,u=0..0.9999999,v=0..2*Pi,shading
> =zhue,
> scaling=constrained, orientation=[50,80]);
> display(top,bot,axes=boxed);
> end:
```

The following command gives the Weingarten surface in Figure 1.

```
> linwein(3,1);
```

The following is the Mylar balloon (see Figure 2).

```
> linwein(2,1);
```

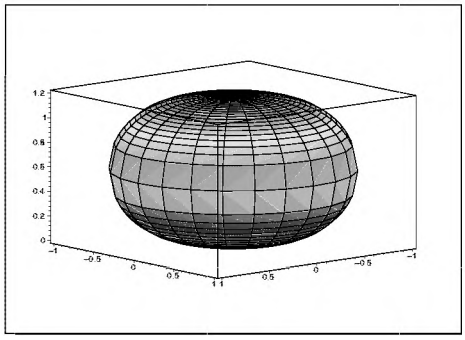

Figure 2. A linear Weingarten surface with $c = 2$: a Mylar Balloon.

9. Weingarten Surfaces in Terms of the Beta Function

While linear Weingarten surfaces are parameterized in Theorem 1 using the hypergeometric function, it is also possible to parametrize them using the Beta function. Here we give this parameterization and relate the Beta and hypergeometric functions.

In fact, we only have to evaluate (44) and for that purpose it is convenient to rewrite it in the form

$$z(u) = \int_u^r \frac{\tilde{u}^c}{\sqrt{r^{2c} - \tilde{u}^{2c}}}\,\mathrm{d}\tilde{u} = \int_u^r \frac{\tilde{u}^c}{r^c\sqrt{1 - \left(\dfrac{\tilde{u}}{r}\right)^{2c}}}\,\mathrm{d}\tilde{u} \tag{45}$$

which suggests that we introduce the variable $t = (\tilde{u}/r)^{2c}$ to immediately obtain

$$\mathrm{d}t = \frac{2c}{r}(\tilde{u}/r)^{2c-1}\,\mathrm{d}\tilde{u}$$

and

$$z(u) = z(t(u)) = \frac{r}{2c}\int_t^1 t^{\frac{1-c}{2c}}(1-t)^{-\frac{1}{2}}\mathrm{d}t. \tag{46}$$

The integral above can however be expressed directly via the **incomplete beta function** which, by definition (see [6], 8.391), is

$$B_\sigma(p,q) = \int_0^\sigma t^{p-1}(1-t)^{q-1}\,\mathrm{d}t. \tag{47}$$

Making use of this definition and taking into account that, in our case $p = \frac{1+c}{2c}$ and $q = \frac{1}{2}$, the integral in (46) can be written in the form

$$z(u) = \frac{r}{2c}\left[B_1\left(\frac{1+c}{2c},\frac{1}{2}\right) - B_\tau\left(\frac{1+c}{2c},\frac{1}{2}\right)\right], \qquad \tau = \left(\frac{u}{r}\right)^{2c}. \tag{48}$$

We can also use Maple to create linear Weingarten surfaces in terms of the Beta function parametrization. First, because Maple does not have an incomplete Beta function, we give a procedure which creates it.

```
> bta:=proc(a,b,x)
> evalf(Int(t^(a-1)*(1-t)^(b-1),t=0..x));
> end:
```

Now, using the `bta` procedure for the incomplete Beta function, we can give a procedure to plot linear Weingarten surfaces given an input c.

```
> lwbeta:=proc(c)
> local p1,p2;
> p1:=plot3d([u*cos(v),u*sin(v),1/(2*c)*(bta((1+c)
> /(2*c),1/2,1)
> -bta((1+c)/(2*c),1/2,u^(2*c)))],u=0..1,v=0..2*Pi,
> scaling=constrained,orientation=[45,70]):
> p2:=plot3d([u*cos(v),u*sin(v),-1/(2*c)*(bta((1+c)
> /(2*c),1/2,1)
> -bta((1+c)/(2*c),1/2,u^(2*c)))],u=0..1,v=0..2*Pi,
> scaling=constrained,orientation=[45,70]):
> display(p1,p2,shading=zgrayscale);
> end:
> lwbeta(2);
> lwbeta(5);
```

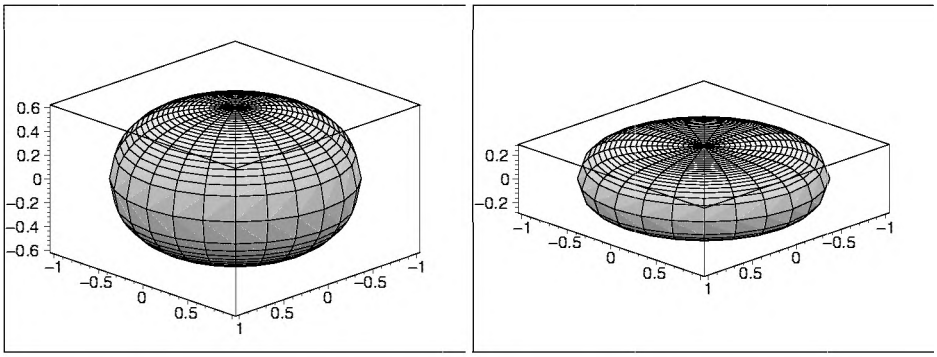

Figure 3. The Mylar balloon and the Linear Weingarten surface with $c = 5$ from the Beta function

10. Geometry of the Deformed Balloons

Once we have the profile curves of the deformed balloons in explicit form, it is an easy task to find some of their geometrical characteristics. For instance, we can

find the relation between the radius r of the inflated balloon and the radius a of disks from which it is constructed by entering with the parameterization (48) in the constraint (40). This gives

$$a = \int_0^r \sqrt{1 + z'(u)^2}\,\mathrm{d}u = \int_0^r \frac{\mathrm{d}u}{\sqrt{1 - \left(\frac{u}{r}\right)^{2c}}} = \frac{B(\frac{1}{2c}, \frac{1}{2})}{2c} r.$$

For a given c, the surface area $A(\mathcal{S}_c)$ is

$$A(\mathcal{S}_c) = 4\pi \int_0^r \frac{u\,\mathrm{d}u}{\sqrt{1 - \left(\frac{u}{r}\right)^{2c}}} = \frac{2\pi B(\frac{1}{c}, \frac{1}{2})}{c} r^2$$

and $\mathcal{S}_c$ encloses respectively a volume V_c which amounts to

$$V_c = 2\pi \int_0^r \frac{u^{c+2}\mathrm{d}u}{\sqrt{r^{2c} - u^{2c}}} = \frac{\pi B(\frac{c+3}{2c}, \frac{1}{2})}{c} r^3.$$

Last, but not least, due to the fact that the beta function is closely connected to the *hypergeometric function* $F(p, q; s; x)$ via the identity (see [1, p. 263])

$$B_x(p, q) = p^{-1} x^p F(p, 1 - q; p + 1, x)$$

all formulas above can be rewritten in terms of hypergeometric functions. On the other hand, our previous results about the Mylar balloon ([10]) were expressed entirely in terms of the elliptic functions and integrals. This means that a number of (potentially new) connections and identities among these functions could be derived. We hope to investigate this further in the future.

Acknowledgments

This work has been partially supported by Bulgarian National Science Foundation under the Contract B-1531/2005.

References

[1] Abramowitz M. and Stegun I., *Handbook of Mathematical Functions*, also available in electronic form from `http://www.math.sfu.ca/~cbm/aands`.

[2] Baginski F., *On the Design and Analysus of Inflated Membranes: Natural and Pumpkin Shaped Balloons*, SIAM J. Appl. Math. **65** (2005) 838-857.

[3] Delaunay C., *Sur la surface de revolution dont la courbure moyenne est constante*, J. Math. Pures et Appliquées **6** (1841) 309–320.

[4] Dwight H., *Tables of Integrals and Other Mathematical Data*, 4th ed., Macmillan, New York, 1961.

[5] Gibbons G., *The Shape of a Mylar Balloon as an Elastica of Revolution*, DAMTP Preprint, Cambridge University, 2006, 7 pp.

[6] Gradshteyn I. and Ryzhik I., *Tables of Integrals, Series and Products*, Academic Press, New York, 1980.

[7] Gray A., *Modern Differential Geometry of Curves and Surfaces with Mathematica*, 2nd ed., CRC Press, Boca Raton, FL, 1998.

[8] Hadzhilazova M. and Mladenov I., *Surface Tension via Cole's Experiment*, In: Proceedings of the Tenth International Summer School of Chemical Engeneering, Sofia, 2004, pp 195–200.

[9] Kühnel W. and Steller M., *On Closed Weingarten Surfaces*, Monatsh. Math. **146** (2005) 113–126.

[10] Mladenov I. and Oprea J., *The Mylar Balloon Revisited*, Am. Math. Monthly **110** (2003) 761–784.

[11] Oprea J., *Differential Geometry and Its Applications*, Prentice Hall, Upper Saddle River, NJ, 1997.

[12] Oprea J., *The Mathematics of Soap Films: Explorations with Maple*, AMS, Providence, 2000.

[13] Paulsen W., *What is the Shape of a Mylar Balloon?*, Amer. Math. Monthly **101** (1994) 953–958.

[14] Yoneda M., *Tension at the Surface of Sea-Urchin Egg: A Critical Examination of Cole's Expariment*, J. Exp. Biol. **41** (1964) 893–906.